

# DEVELOPMENT OF HARMONIC FIELD MEASUREMENT SYSTEM WITH HIGHER RESOLUTION ADC

R. Kitahara, Y. Fuwa, Y. Iwashita, Y. Nasu  
ICR, Kyoto University, Kyoto, Japan

## Abstract

Quadrupole magnets for ILC final focus should be strong enough with the restriction on the external radius, while vibration of the magnetic center has to be highly avoided to keep the nm sized beam focusing stable at the interaction point a few meter downstream from the lens. Gluckstern's 5-ring PMQ singlet seems a good candidate for the purpose. The precise magnetic harmonic field measurement system is developed for adjusting each magnet ring and evaluation of the assembled singlet. A rotating magnet system and a rotating coil system are prepared for the former and the latter purposes, respectively. Both systems have 24-bit ADCs for higher resolution. For the rotation coil, a flexible print circuit sheet, which has a pair of printed one turn coils, is glued on a quartz rod. The two coils located on the quartz rod with the angle difference of 180 degree can separate the odd and even harmonics components by recording both the signals of their sum and difference. The two digitized signals are numerically on the rotator side and the digitized data are transferred to the ground for recording.

## INTRODUCTION

Magnetic multipole field plays an important role in beam optics. For example, quadrupoles are used for focusing beams, and sextupoles or octupoles are used for correcting non-linear or chromatic aberration. Sextupole magnetic fields focus cold neutron beams through the neutron's magnetic dipole moment.

In the final focus system of International Linear Collider (ILC), electron and positron beams are focused in nm order size to collide with a crossing angle 14 mrad. The outer diameter is limited so that the beams that passed through the interaction point have to run through the outsides of the final focusing magnets. We fabricated the prototype system of the final focus lens by permanent magnets (PM)[1], which has less micro vibration and smaller size compared with superconducting magnets. Possible x-y coupling terms in beam transfer matrices can be suppressed by Gluckstern's 5-ring PMQ's relative rotation.

## SET UP

### Principle of harmonic coil

In beam optics, it is effective to use coordinate system that beam direction is parallel to z axis (see Fig. 1). A radial component of magnetic flux density B on the shaft surface of radius R, is expressed by

$$B_r(\theta, z) = \sum_{n=1}^{\infty} b_n(z) R^{n-1} \sin(n\theta + \alpha_n) \quad (1)$$

Therefore magnetic flux  $\Phi$  that crosses the coil is expressed by

$$\begin{aligned} \Phi(\theta) &= \int_{z_1}^{z_2} \int_{\theta_1}^{\theta_2} B_r(\theta, z) \cdot R d\theta \cdot dz \\ &= -2 \sum_{n=1}^{\infty} \frac{b_n R^n}{n} \sin\left(n \frac{\Delta\theta}{2}\right) \cos(n\theta + \alpha_n) \end{aligned} \quad (2)$$

where  $n$  is a harmonics number,  $\theta$  is a coil angle,  $\alpha_n$  is phase angle of  $n$ -th component,  $b_n = \int_{z_1}^{z_2} b_n(z) dz$  is an integrated component of  $n$  along the axis, and  $\Delta\theta = \theta_2 - \theta_1$  is the opening angle of a coil.

When a harmonic coil rotate in multipole magnetic field, electromotive voltage V through the coil is expressed by

$$\begin{aligned} V(t) &= \frac{d\Phi}{dt} \\ &= 2 \sum_{n=1}^{\infty} \frac{b_n R^n}{n} n\omega \cdot \sin\left(n \frac{\Delta\theta}{2}\right) \sin(n\omega t + \alpha_n) \end{aligned} \quad (3)$$

$\omega t = \theta$ ,  $\omega$  is an angular velocity,  $t$  is elapsed time. The Voltage is usually integrated over the time to eliminate the effect of the fluctuation of the rotation speed, where the sample timing pulses are given by a rotary encoder. Instead of integrating the voltage all over the measurement time, we reset the integration at each encoder pulse for continuous measurement. Then the magnetic flux at time  $t$  ( $=k \Delta t$ :  $k=0, 1, 2, \dots$ ) is expressed by

$$\begin{aligned} \Phi_n &= \int_{t-\frac{\Delta t}{2}}^{t+\frac{\Delta t}{2}} V(t) dt \\ &= 4 \sum_{n=1}^{\infty} \frac{b_n R^n}{n} \sin\left(n \frac{\Delta\theta}{2}\right) \sin\left(n\omega \frac{\Delta t}{2}\right) \cos(n\omega t + \alpha_n) \end{aligned} \quad (4)$$

where  $V(t)$  is integrated by a range of sampling rate  $\Delta t$ . The Fourier component  $F_n$  of flux  $\Phi_n$  is expressed by

$$F_n = \frac{1}{N} \sum_{k=1}^N \Phi_k e^{ikn \frac{2\pi}{N}} \quad (5)$$

where  $N$  is the number of rotary encoder pulses per turn. Therefore from Eqs. (4) and (5), the magnetic field harmonic components  $b_n$  are derived by,

kitahara@kytier.kuicr.kyoto-u.ac.jp

$$b_n = \frac{F_n}{\kappa_n}, \kappa_n = \frac{2R^n \sin\left(n \frac{\Delta\theta}{2}\right) \sin\left(n\omega \frac{\Delta t}{2}\right)}{n}$$

where  $\kappa_n$  is a constant coefficient for each  $n$  which depends on the magnification of circuit and coil form factor.

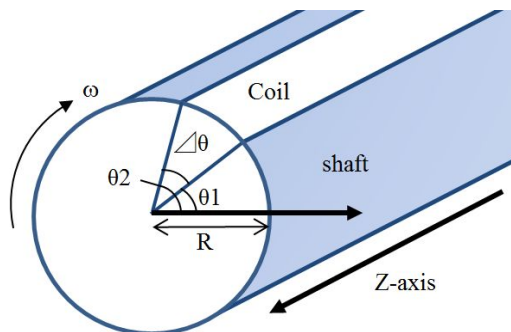


Figure 1: The coordinate system of the shaft.

*Structure of harmonic coil*

Material of the shaft is quartz which has a low thermal expansion coefficient. The diameter is 13 mm and the length is 60cm. The both edges are supported, one of which is connected to a pulse motor (see Fig. 2). A typical angular velocity of the pulse motor is  $2\pi$  rad/s. A pair of one turn tangential coil whose longitudinal length is 30 cm is located on the shaft with an angle of 180 degree apart. Three opening angles are available from the combination of three terminals, among which appropriate one should be used for harmonic components to be measured (see Fig. 3). For example, if the angle  $\Delta\theta/2$  meet  $1/6$ ,  $b_6$  component is very small signal. The max angle of our system is  $\pi/7 + \pi/12$  and then we can measure the enough signal amplitude (i.e.  $n=1, 2, 3$ ). A 3-axis moving stage can position a target magnet against the coil.

*Electric circuit*

Figure 4 is a block diagram of the electric circuit. A gain of PGA (Programmable Gain Amplifier) can be selected according to the size of the analog signal from a coil. After PGA, the signal is digitalized by a  $\Delta-\Sigma$  type 24 bit high resolution ADC(AD7765) whose sampling rate is fixed at 156250 Hz. The sampled data between  $\Delta t$  is numerically integrated in the control circuit. The timing of the sampling points does not synchronize with the rotary encoder pulse edges. The start and end data points of integration are respectively interpolated from closest two sampling data points of ADC. A numerical integration overflow that is usually caused by an offset of amplifiers is not a matter because  $\Delta t$  is short enough. Thus the system can be measurement. The measurement starting point is given by z-pulse of the rotary encoder. The resolution of the rotary encoder is 8192 Hz pulses per rotation, while the number of integrated data points can be selected from 1024 and 8192.

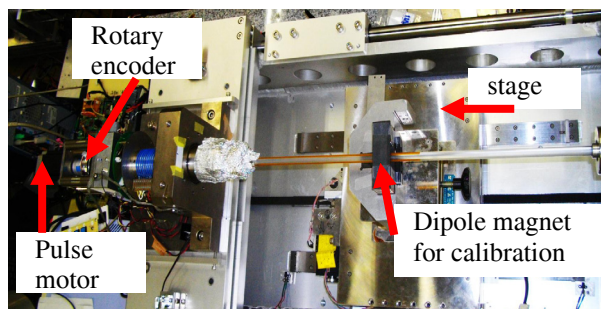


Figure 2: Top view of the harmonic coil system.

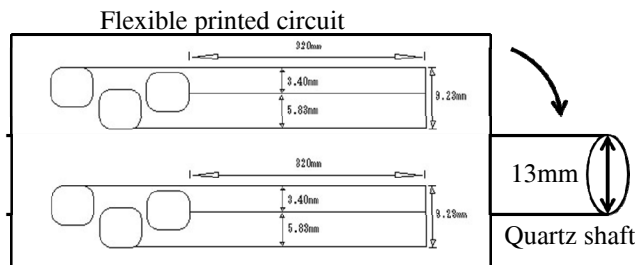


Figure 3: Two one turn coils on a flexible printed circuit is glued on the shaft. The coil has three legs. Copper foil's thickness is 35  $\mu$ m and the width is 100  $\mu$ m. The sheet circuit thickness is 25  $\mu$ m.

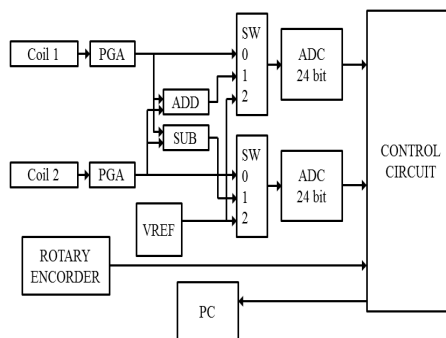


Figure 4: The Block diagram of the electric circuit. The system can get a sum and a difference data between coil 1 and coil 2. It is useful to separate multipole components with large magnitude ratios.

**EVALUATION OF SYSTEM**

*Background noise*

With data for eight terms in one measurement, a harmonics number obtained from a Fourier transformation should be scaled down to 1/8. Only integer harmonics components are meaningful (see Fig. 5), because of the periodicity. Non-integer components are considered as background noise for a measurement because they don't meet periodicity requirement. This noise might be caused by an electric noise, the amplifiers, or a mechanical noise such as a vibration of the shaft.

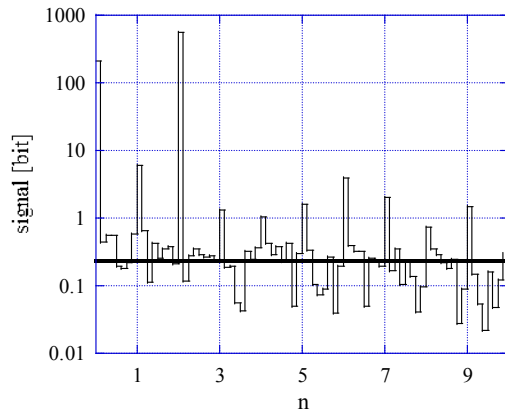


Figure 5: Fourier components of a Q-magnet for a calibration of harmonic coil system. Black horizontal line is a mean value of non-integer components.

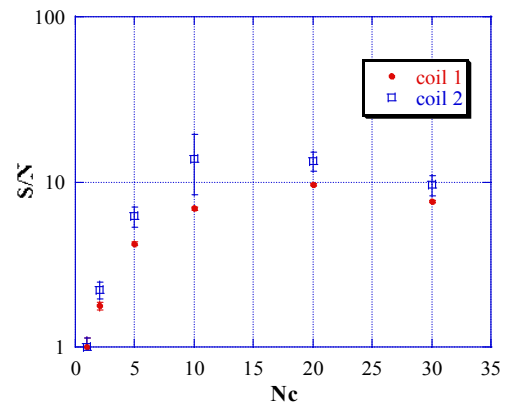


Figure 6: S/N ratio every  $N_c$ .

**Calibration**

There is a following relation between the obtained signal values  $V_{signal}$  and a flux  $\Phi_{sample}$  supposed to be measured,

$$\Phi_{sample} = \int V(t)dt = \frac{\alpha}{x} \times \frac{V_{signal} \times \Delta t'}{(N_c)} \quad (6)$$

where  $x$  is a gain of PGA,  $\alpha$  is a coefficient between voltage and binary data (V/bit) and  $N_c$  is number of terms for a measurement. For example, in case of  $N_c=5$ , measured data are summed up for five sets,  $8 \times 5=40$  rotation measurement, and become the average data for five sets by dividing by  $N_c$ . Fig. 6 shows the  $N_c$  dependence of the background noise. The S/N ratio seems to saturate after  $N_c=10$ . The background noise may have components synchronizing to the rotation.

From 2D magnetic field mapping of D-magnet and Q-magnet by hall probe,  $b_n$  of each  $n=1, 2$  were available and  $\alpha$  was calibrated by as  $1.49 \pm 0.03E-9$  and  $1.51 \pm 0.04E-9$  for coil 1, 2, respectively.

**Position precision of Coil glued on the shaft**

Two attracted Neodymium magnet pieces create the dipole magnetic field locally with bringing a joint close near the rotating coil (see Fig. 7). The measured data had two pairs of (positive and negative) peaks, which corresponds to two wire position of a coil (see Fig. 8). The distance between the first negative peak and the third positive peak corresponds to the opening angle  $\Delta\theta$  and the peak height depends on relative radial distance  $\Delta R$ . By moving the position of the magnet from  $Z=3$  cm to  $Z=30$  cm the data were recorded every 3 cm with maximum  $\Delta\theta$ . It shows that the deviation of the angular position of the glued coils are  $\pm 50$  mrad for coil 1 and  $\pm 100$  mrad for coil 2 and those of the radial position from the shaft surface are about 200  $\mu m$  for coil 1 and 100  $\mu m$  for coil 2.  $\Delta\theta$  fluctuations are as wide as the line width of copper wire on the flexible print circuit.

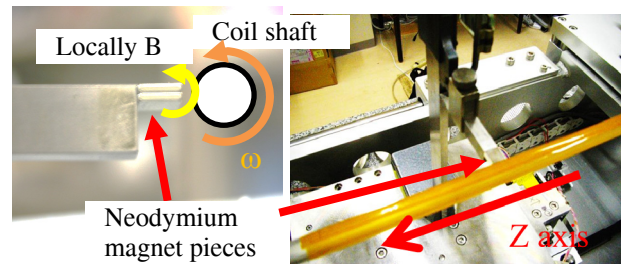


Figure 7: A view of setting measurement of precision of coil glued on the shaft.

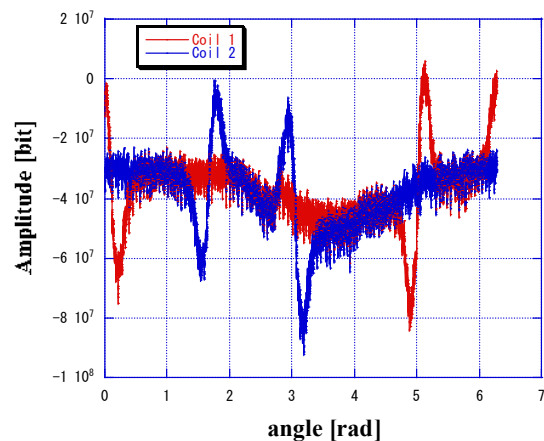


Figure 8: A raw data of measurement of localize dipole magnetic field at  $Z=xx$  cm.

**REFERENCES**

[1] Y. Iwashita, H. Fujisawa, M. Ichikawa, H. Tongu, S. Ushijima, "Beam Test Plan of Permanent Magnet Quadrupole Lens at ATF2," IPAC'10, Kyoto, June 2010, WEPE017, p. 3380 (2010); <http://www.JACoW.org>